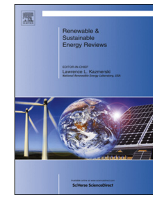
Renewable and Sustainable Energy Reviews 33 (2014) 323–332

Contents lists available at ScienceDirect

Renewable and Sustainable Energy Reviews

journal homepage: www.elsevier.com/locate/rser



Lighter-than-air particle velocimetry for wind speed profile measurement

Jesús Gonzalo [a], Diego Domínguez [b], Deibi López [a], Joaquín Fernández [c,*]

[a] Universidad de León, Aerospace Engineering Area, Campus de Vegazana s/n, 24071 León, Spain
[b] Vrije Universiteit Brussel, Department of Engineering Technology, Campus Kaai, 1070 Brussels, Belgium
[c] Universidad de Oviedo, Hydraulic Area, Campus de Barredo s/n, 33600 Mieres (Asturias), Spain

ARTICLE INFO

Article history:
Received 24 January 2013
Received in revised form
11 January 2014
Accepted 31 January 2014
Available online 3 March 2014

Keywords:
Anemometry
Atmospheric boundary layer
Particle image velocimetry
Wind measurement
Wind profile

ABSTRACT

The objective of this paper is to consolidate the backgrounds of a method to measure the local wind speed profiles by remotely tracking lighter-than-air bubble clusters, in a way that is efficient, safe and easily implementable. The technologies around remote sensing of atmospheric wind profiles are reviewed, together with those associated with particle image velocimetry. In this case, the targets are light liquid bubbles filled with helium, which are monitored from several locations on ground so that the full trajectory can be reproduced and hence, the wind speed derived at each point along the path. The features of the measurement system are detailed, describing its major components. The different applicable data filtering processes, the core of the operation, are reviewed to find the best options for the estimation of the wind profile in real time. The capability to measure the horizontal wind along the ascending path of the targets has been checked by means of simulated scenarios, indoor campaigns and in-field tests. The synthetic scenarios allowed the tuning of photometric parameters as well as the first estimation of the performance and the limitations. The field test campaigns allowed validating the prototype under different configurations and atmospheric conditions. Initial tests were conducted in a Spanish atmosphere research centre (CIBA), where wind data until 100 m height is continuously recorded, followed by additional experiments in a more realistic environment, near an airport, where these data could be operationally used in the future. The results from these tests are successful, taking into account the fact that the system is still in an early development phase, while still being able to beat initial performance goals (0.4 m/s mean error for wind speed and 15° for wind direction). It is expected that the idea is a reliable and low cost alternative to other remote sensing devices for wind profile measurement in certain applications in the medium-accuracy range.

Contents

* Corresponding author.
E-mail address: jffrancos@uniovi.es (J. Fernández).

http://dx.doi.org/10.1016/j.rser.2014.01.082

1. Introduction

There are many activities that require a good knowledge of wind speed profiles in the lower part of the atmosphere, like wind energy production, civil engineering, pollutant dispersion or pedestrian comfort amongst others [1–4].

The study of wind speeds and directions is not an easy task, especially if the region of interest is close to the ground because the viscosity governs the air movement near flow boundaries. For the Earth's surface, the boundary layer can be as high as 1000 m over the terrain, changing the wind speed from zero to geostrophic winds [5]. Furthermore, the wind changes its direction with height due to Coriolis forces [6]. Efforts to model the wind speed profile in compact formulations have been continuous over a long period of time, ending up with different mathematic models, the most popular of which is the logarithmic law corresponding to an atmospheric neutral condition, being deduced from a similarity study [7].

But when higher accuracy in the boundary layer knowledge is needed, the standard logarithmic law and its variations are not enough; for the last few decades, new systems have been developed to measure the wind speed values close to the surface. Meteorological towers, LIDAR, RADAR, SODAR, observation balloons or satellites are some examples of these kinds of systems [8].

Meteorological towers are probably the most common resource for measuring the wind speed and direction at a specific place. They are tall (between 40 and 120 m height) and precise, because wind speed and direction can be measured using anemometers and wind vanes at different heights after rigorous calibrations.

RADAR (Radio Detecting and Ranging) can measure the wind velocity by means of the reflection of electromagnetic waves from rain drops, hail or snow. The Doppler velocity is estimated from the phase shift between the return signals of consecutive transmitted pulses [9]. Its limitations are mainly due to anomalous propagation of electromagnetic waves, ground clutter or non-natural interferences like wind farms [10]. There are also limitations on the spatial resolution achieved.

Light Detection and Ranging (LIDAR) uses the reflection of light pulses. This allows high spatial and temporal resolution of the measurements from the ground to more than 100 km, obtaining several atmospheric variables such as temperature, pressure, humidity and, of course, wind speed and direction [11]. Its efficacy has been demonstrated in several applications like measurement of aircraft true airspeed, detection and tracking of clear air turbulence, wind shear, gust fronts, aircraft wake vortices and of course the capture of full atmospheric wind profiles [12].

Sound Detection and Ranging [SODAR] is based on the reflection of sound waves to detect the wind speed and direction at various elevations above the ground [13]. Being more affordable than RADAR and LIDAR systems, one of the most important problems with SODAR is ground clutter, which can severely influence and disturb the echoes. Furthermore it must be located far away from populated locations [14].

Observation balloons have been used for gathering meteorological data for centuries. A lighter-than-air balloon with some meteorological instruments collects data from the desired variables of the atmosphere. Releasing many balloons at the same time allows the acquired data to be compiled into a single scenario at a certain point of time [15]. Also, it the vehicle is large enough, it is possible to include a radar reflector to better measure the wind properties by tracking it from the ground [16].

Satellites are also a valuable tool used to monitor and forecast the movement of air around the globe because they can provide cloud remote sensing and good profiles of temperature and moisture at different levels in the atmosphere by means of special radiometers called sounders [17]. However, measuring wind speed from space is more difficult and there only exist two ways: wind scatterometers [18] and LIDAR devices like Doppler Wind LIDAR [19].

Each technology has its own advantages and drawbacks, many times related to the cost of the equipment or problems with the deployment and installation. For example, should critical locations like airports be the scenarios of interest, where there are severe restrictions related to safety and the height of the structures near the runway is very limited, some of the systems will need to be discarded. The method analysed in this paper is a scaled version of the technique employed with weather balloons, which are usually tracked by radar, radio direction finding or navigation systems in order to obtain wind data from the ground to several kilometres high.

Also, some ideas are borrowed particle image velocimetry (PIV) techniques, where fluid velocity is calculated by measuring the velocity of tracer particles tracked from optical cameras [20]. The most popular technique is the 2D PIV [21,22] although during the last few years more work has been done by capturing the three-dimensional flow fields with a volumetric particle-image velocimetry system (V3V) [23,24]. Like in PIV, the fluid contains small particles which should follow the flow in a good manner. Three sensitive cameras capture the laser light reflected by the tracing particles within a short time interval. Based on the displacements of each particle and the time between the recordings, the velocity of all particles in the measurement volume can be determined. A critical issue to apply this technique is being able to feed the flow in the right way, having an adequate number of tracer particles in the measurement region (the resulting reflection fields should ideally contain about 70,000 source particles [25]). Because of this, PIV techniques are usually limited to enclosed flows with limited test sections.

The bubble tracking method, although inspired by these techniques, has been designed to be used in open air to measure atmospheric boundary layer profiles and some preliminary results have been obtained with this technique in a recent work [26]. Also recently, a similar but more complex and expensive method that consists of small, helium-filled tracer balloons and an instrument that tracks them with high spatial resolution by means of a LIDAR rangefinder has been developed and tested [27]. This method proved to be useful when measuring horizontal wind speed, wind direction, and vertical shear. On the other hand, and also applying a bubble tracking technique, [28,29] are developing a system to quantitatively measure wind flow near the ground surface in both the horizontal and vertical directions (in other words, wind flow in three dimensions) using photogrammetry. In this method, a balloon (a no-lift balloon), with the same relative weight as air, and soap bubbles were released as tracers. The results of the testing proved that the measurement methods were effective.

The initial objective, based on a manual prototype for the bubble generation, is to achieve better accuracy than 0.4 m/s average for wind speeds and 15° average for wind direction in the first 30 m of height. Accuracy using two or three cameras for the bubble tracking is also compared. In further developments, new calibration procedures can be included during the post-processing with the aim of reducing measurement errors to 0.15 m/s and 6°.

In summary, the research work is focused on the development of an affordable wind profile measurement system, which should be able to provide accurate knowledge of the local wind speed profiles by remotely tracking lighter-than-air bubbles. The goal is to achieve a reliable and low cost alternative to the previously referred methods for certain conditions and applications.

2. System overview

The system concept is quite simple and derived from particle image velocimetry techniques. In this case, remote optical sensors

track lighter-than-air bubbles, which can move freely through the atmosphere only pushed by the aerodynamic force and its own buoyancy and weight. Thanks to their negligible mass/inertia, it is possible to deduce horizontal wind speed directly from bubble speed. A brief description of the system is included here and a more detailed one can be found in [30]. The concept of 'bubble cluster' or 'conglomerate' is used in the paper to refer to a single compact target, formed by thousands of micro-bubbles (1–3 mm) and with sizes in the range of tenths of centimetres and hence easily observable.

2.1. General description

The most convenient sensors for the bubble cluster tracking are optical cameras, due to their relative low cost and currently available high performance. Bubble clusters are a good target because they are harmless for airplanes or people, very cheap and not hazardous to the environment. The system envisaged has four mean elements:

1. A tracking camera, whose goal is provide bubble cluster pictures frequently with enough contrast to resolve its location.
2. A bubble generator, producing bubble clusters whenever the control centre commands it.
3. A bubble cluster, a conglomerate of bubbles made with a solution of soap, glycerine and water and filled with helium. A complete explanation of bubble properties and how to make them is given in [31].
4. A control centre, analysing images, identifying bubble clusters and measuring their elevation and azimuth. All these elements, as well as their distribution and organisation, are depicted in Fig. 1.

2.2. Data acquisition process

The core of the system is the data handling and processing, a critical task in order to achieve accurate and reliable estimates in real time. The best estimate of the bubble position and velocity at every moment is that which smartly uses all the information available at that time, e.g. the system dynamics and its fidelity, the sensor measurements and their expected accuracy, the starting conditions and other parameters involved in the problem.

During the last few decades, the Kalman filter [32] was present in most of the data smoothing problems as it presents unbeatable advantages. On one hand, the filter is optimal, that is to say it looks for the best fit amongst available sensor readouts and the expected system behaviour given by its dynamics. This is performed by including in the formulation the sensor errors, the estimated system noise (as one is not able to perfectly model the reality) and the history of the whole process. The term optimal implies that the global error, the output of the filter with respect to the real world state, is minimum under conventional assumptions on the noise probability distributions. On the other hand, the algorithm is easily manageable by computers, as it adapts very well to discrete forms, not requiring a lot of storage because all the history is captured in few parameters which are updated at every algorithm step.

The Kalman algorithm is a recursive prediction–correction process, where the system state is propagated in time together with noise covariance, in such a way that the filter is, at every time, weighting the importance of the next state given by the sensors and the one obtained by the system dynamics to provide the best estimate for the next time.

However, some filter constraints are noticeable. Mainly, the fact of being a linear filter requires simplifications of the system dynamics and the measurement functions by using Taylor series first terms. Extensive literature focuses on how to manage this issue, which is more problematic as the dynamics is more aggressive. The first approach (Extended Kalman Filter, EKF) is to use non-linear functions for those terms in the formulae which allow for a better prediction phase [13]. Unfortunately, the noise covariance terms still need a linearization of the expressions, using the Jacobian, which sometimes are still inaccurate. This leads to other developments for the covariance calculation/propagation such as the unscented Kalman, the ensemble Kalman and other filters [33]. On top of that, there are numerous variations to accommodate the particular problems, playing with the time discretisation and the way to include constraints, mainly in the correction phase of the algorithm. Furthermore, there is a new class of solutions to provide estimations and dataset smoothing that could be more suitable to non-linear problems but involves much more processing complexity as any kind of Sequential Monte Carlo method [34].

One of the beauties of the Kalman filter is that, even when only position sensors are involved, the velocity is an output of the filter. In the case of the lighter-than-air bubble tracking, this is an advantage as wind velocity estimation is the final goal.

Each tracking camera is located in a fixed and known location, providing pictures that immediately provide azimuth and elevation of each target. These are obtained by means of a coordinate transform equation set following Fig. 2, tuned by a calibration campaign to cope with optics aberrations. Thus, as bubbles are progressing, a sequence of azimuth and elevation data is measured. Currently, the recognition of the object on the image is performed in a semi-automatic manner, with an algorithm that, once scaled for certain illumination conditions, is able to track the

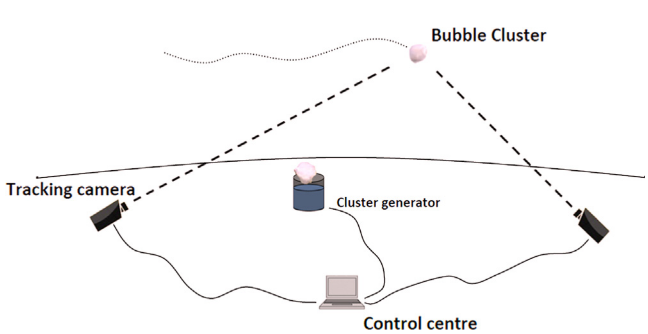


Fig. 1. Description of the wind speed profile measurement system.

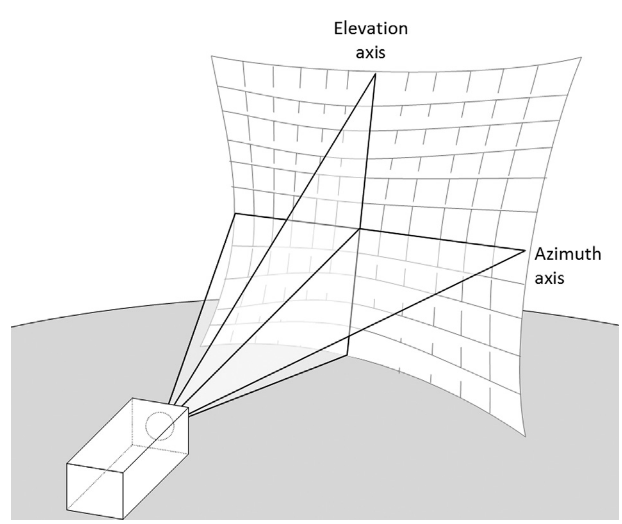


Fig. 2. View of the camera geometry to determine target position.

centroid of the bubble cluster along its way. The error in such measurements (ε) is assumed to be isotropic, independent, white, with normal probability distribution, zero mean and covariance R and it is a function of the electro-optical configuration of the detector (element pitch and focal length). Knowing the angular positions, logic states that the position and velocity of the bubble cluster can be estimated by a triangulation process if at least two cameras are available. Given their slow dynamics, the most suitable tool for this process is the EKF, which allows the use of azimuth/elevation pairs that do not exactly match a single point in the air (due to sensor errors) to provide the best estimation of the position of the bubbles, as well as their speed, in a single integrated process.

Considering the EKF, the following equations apply:

- Time update equations (prediction):

$$x_{(t+1|t)} = \Phi x \tag{1}$$

$$P_{(t+1|t)} = \Phi^T P_{(t|t)} + Q_{t+1} \tag{2}$$

- Measurement update equations (correction):

$$K_{t+1} = P_{(t+1|t)} H_{t+1}^T (H_{t+1} P_{(t+1|t)} H_{t+1}^T + R_{t+1})^{-1} \tag{3}$$

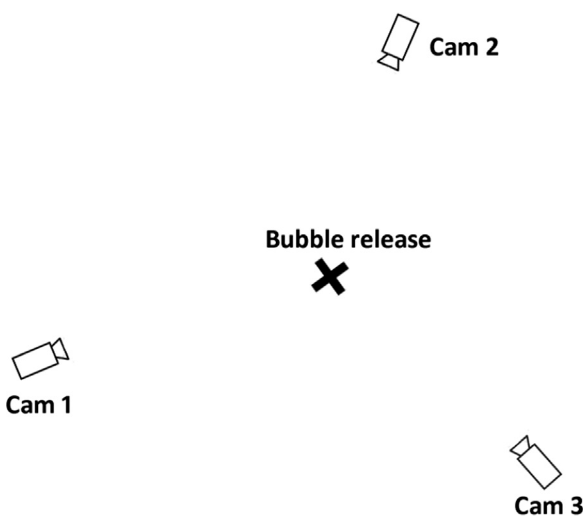


Fig. 3. System architecture for three cameras.

$$x_{(t+1|t+1)} = x_{(t+1|t)} + K_{t+1}[z_{t+1} - h(x_{(t+1|t)})] \tag{4}$$

$$P_{(t+1|t+1)} = (I - K_{t+1} H_{t+1}) P_{(t+1|t)} \tag{5}$$

where

- x: state vector $x=[x, y, z, vx, vy, vz, az]$, where the vertical acceleration is not considered system noise but a non-negligible value that needs to be measured and maintained along the filtering process, as a result of some test campaigns focused on the initial behaviour of the cluster after release.
- Φ: state transition matrix between two consecutive states

$$\Phi = \begin{bmatrix} 1 & 0 & 0 & \Delta t & 0 & 0 & 0 \\ 0 & 1 & 0 & 0 & \Delta t & 0 & 0 \\ 0 & 0 & 1 & 0 & 0 & \Delta t & \frac{\Delta t^2}{2} \\ 0 & 0 & 0 & 1 & 0 & 0 & 0 \\ 0 & 0 & 0 & 0 & 1 & 0 & 0 \\ 0 & 0 & 0 & 0 & 0 & 1 & \Delta t \\ 0 & 0 & 0 & 0 & 0 & 0 & 1 \end{bmatrix} \tag{6}$$

- P: error covariance matrix
- Q: process noise matrix
- R: measurement error covariance matrix, defined by sensor variance σ^2 (Grewal and Andrews [36])
- K: optimal Kalman gain for the update process
- H: Jacobian of the measurement function $h(x)$, containing the trigonometric functions to translate from system state variables to the measured angles given by the cameras.

An important feature of this system is its scalability, which provides important advantages. Along the work presented in this paper, this concept has been proved, making the system work with three cameras instead of the usual two, in order to analyse the operational advantages and performance improvements that could be achieved. It was already stated in previous works that hardware and numerical codes can be easily adapted to include more tracking cameras, as the filter properly weights their measurements into the final result. Only three elements from the EKF need to be slightly modified when including a third camera: observation vector z now includes six angular values instead of the usual four, matrix R includes two new elements with the third camera variance and, finally, the measurement function h and its Jacobian should be expanded to accommodate two new elements referring to the additional camera. The formulae employed in the additional elements are completely equivalent to those already used for cameras 1 and 2. The location of the



Fig. 4. An example of bubble clusters identified in a photograph.

cameras surrounding the bubble cluster generator is depicted in Fig. 3; should a-priori knowledge of the wind direction be known, the location can be optimised as the best results are obtained when the three lines of sight are independent.

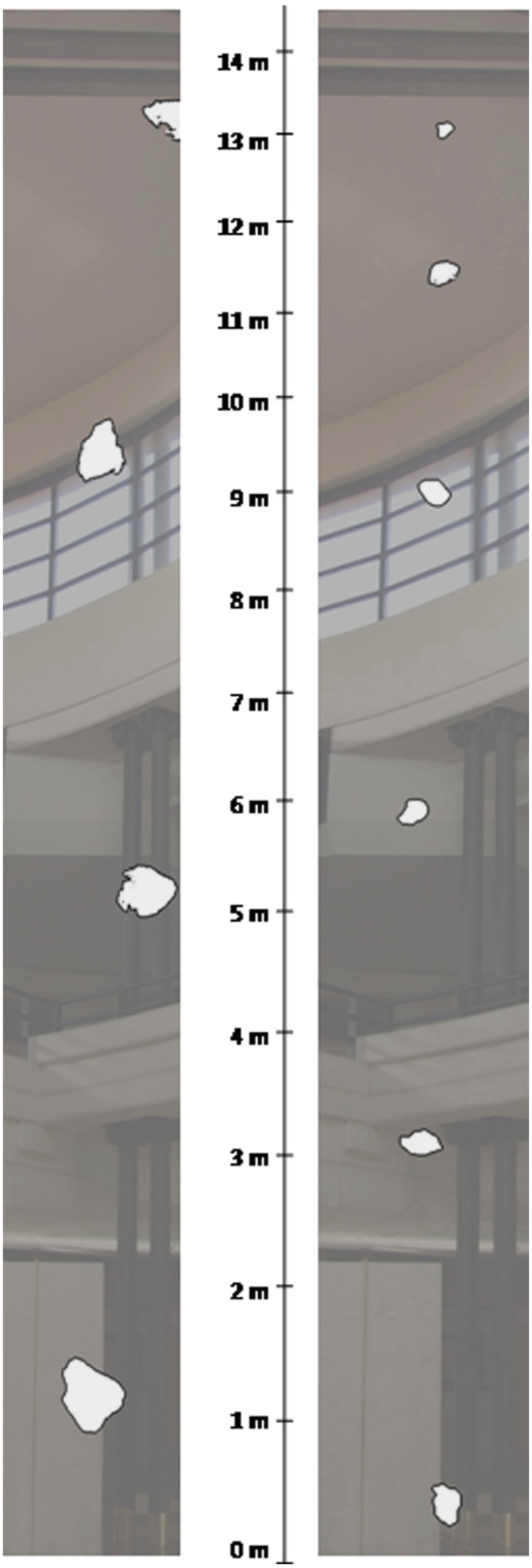


Fig. 5. Large and small bubble clusters processed for the calculation of the position and speed.

3. Field test campaigns for preliminary validation and verification

Prior to field tests, basic system performance was already tested by means of numerical simulations. This initial work

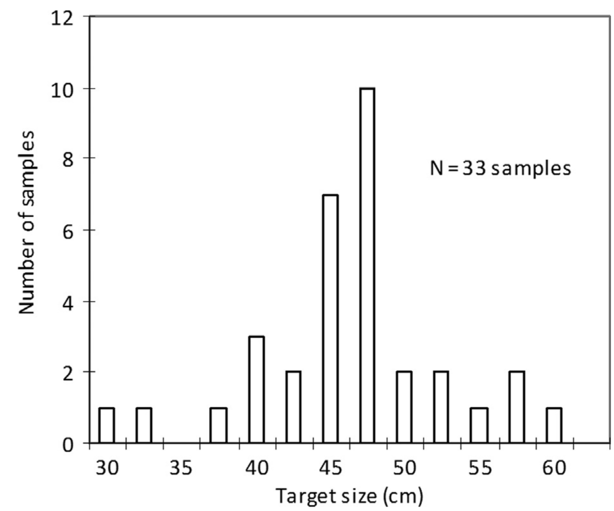


Fig. 6. Histogram of bubble cluster sizes during indoor tests.

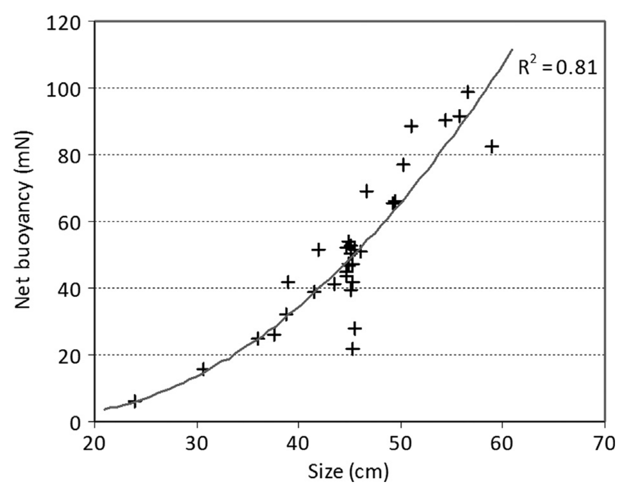


Fig. 7. Net buoyancy as measured before release.

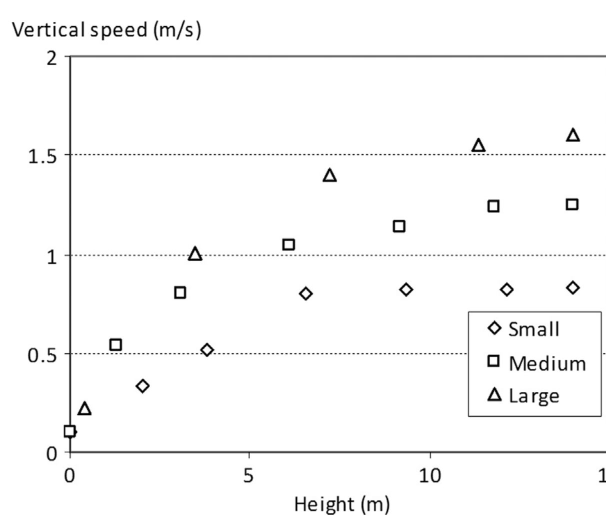


Fig. 8. Vertical speed of ascending bubbles classified by size.

provided valuable data about important characteristics related to filter configuration, temporal resolution or optimum locations for system components [30].

Following the results of the simulated data, a prototype system was constructed in order to be deployed during in-field tests. The equipment includes a prototype version of the bubble generator and three high resolution (10 Megapixels) commercial photographic cameras (Canon PowerShot SX110 IS, 35 mm focal length and 0.78 frames per second). Also, a computer and an ultrasonic anemometer with its own support structure were required when there were no other measurement systems available. These elements allowed the generation and tracking of bubble clusters that can be easily identified in pictures, even when they are taken at a distance longer than 200 m. The bubbles are formed by injecting pressurised helium in a container with water, soap and glycerine. The individual bubbles, with typical sizes of 1–3 mm, join together to form large conglomerates or the so-called clusters of bubbles (as easily appreciated in Fig. 4).

The in-field test campaigns were designed in such a way that the system was operating under different atmospheric conditions as well as at different locations. For example, in the airfield, wind conditions vary quite a lot on a sunny day, as sun heats the surface of the terrain and buoyancy effect has a great influence on the planetary boundary layer.

3.1. Indoor experiments

In parallel with the setting up of the field campaign, a group of indoor experiments was carried out to understand the bubble cluster behaviour when freely released in the atmosphere, mainly in relation to the effect of the ascending speed and their dependence on the size of these lighter-than-air targets. The bubble generator was installed in a location with up to 15 m of clear ascending path, in an area with an altitude similar to the airfield and hence with representative atmospheric conditions.

Bubble clusters were generated, measured for buoyancy and manually released while a calibrated camera (Fig. 5) tracked their vertical trajectories. Up to 33 targets were analysed, with sizes in a 30–60 cm range and a distribution as shown in the histogram of Fig. 6. The measured buoyancy, taken by a precision scale, followed a well-behaved cubic curve as shown in Fig. 7, because bulk buoyancy is proportional to the volume (cubic power of longitudinal size) as well as the soapy water and helium weight. The fit meets a Pearson R^2 of 0.81, which is considered acceptable as the bubble size range is large. It must be noted that although the size of the cluster is variable, the bubbles maintain a shape and size (small) that is very stable during all the tests and hence the only difference amongst clusters is the number of bubbles inside.

Once released, bubble clusters accelerate along their accession (Fig. 8) while the camera is taking pictures, which are immediately processed in a semi-automated algorithm to extract the exact position of the cluster centroid at the measurement time, every 1.56 s. The targets quickly reach their limit velocity, the value, time and position of which are dependent on the cluster size as shown in the example of Fig. 9.

The reason is that the aerodynamic force, towards the ground, increases with the square of the relative velocity. Besides, this force is proportional to the frontal area in such a way that, when compared to buoyancy, small clusters are penalised with respect to larger ones, which can travel more rapidly. Clusters were classified into three classes: small ($<$ 40 cm), medium/typical (between 40 and 50 cm) and large ($>$ 50 cm). The obtained limit velocities range from 0.8 m/s (small) to 1.6 m/s (large).

Given the above results, the consideration of a vertical acceleration makes sense to improve the accuracy in the first few seconds of the target trip. Values around 0.1 m/s^2 are typical; a maximum value of 0.35 m/s^2 was reported during the initial trip of a big cluster.

With respect to the mass, the figures obtained from the buoyancy measurements allow one to estimate typical cluster masses in the range 6–9 g. Even though these figures need to be increased, in the dynamic models, with virtual masses to account for the work developed towards the displaced air, the values are small enough to

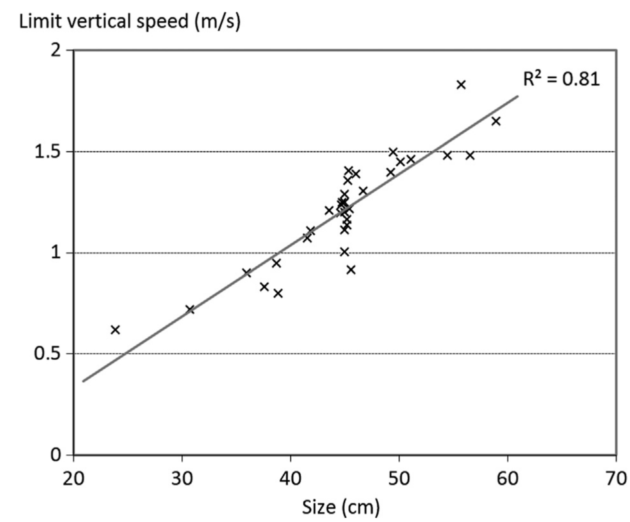


Fig. 9. Limit vertical speed of ascending bubbles.

Table 1
Comparison between anemometer and bubble tracking results for wind speed. Test site: CIBA.

Test	1	2	3
Date	02-04-2013	03-04-2013	12-04-2013
Time (local)	12:35	10:50	13:35
Height 2.2 m			
Anem. (m/s)	6.76	6.51	5.72
Bub. (m/s)	6.52	6.00	5.80
Rel. error (%)	3.55	8.29	1.40
Height 9.6 m			
Anem. (m/s)	8.48	8.03	7.36
Bub. (m/s)	8.02	7.95	7.92
Rel. error (%)	5.42	1.00	7.61
Height 34.6 m			
Anem. (m/s)	10.45	9.56	9.99
Bub. (m/s)	NA	9.90	9.71
Rel. error (%)	–	3.56	2.80

Table 2
Comparison between anemometer and bubble tracking results for wind direction. Test site: CIBA.

Test	1	2	3
Date	02-04-2013	03-04-2013	12-04-2013
Time (local)	12:35	10:50	13:35
Height 2.2 m			
Anem. (deg)	NA	NA	NA
Bub. (deg)	–	–	–
Dif. (deg)	–	–	–
Height 9.6 m			
Anem. (deg)	44.4	41.5	36.5
Bub. (deg)	53	47	46
Dif. (deg)	−8.6	−5.5	−9.5
Height 34.6 m			
Anem. (deg)	51.8	47.5	38.5
Bub. (deg)	NA	38.5	30
Dif. (deg)	–	9.0	8.5

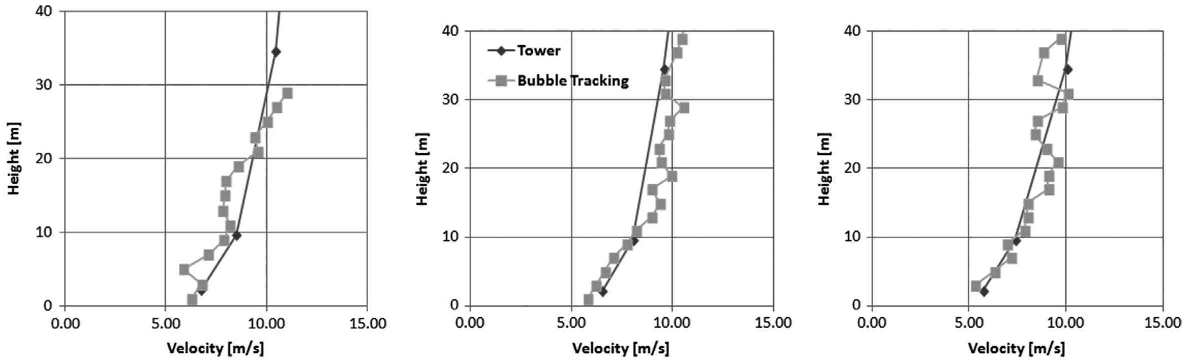


Fig. 10. Wind profiles measured by anemometers in the tower and the bubble tracking system.

Table 3
Results from the test conducted at CIBA at 15:00 – 02/04/2013.

Height (m)	Tower measurements (m/s)	Results from three cameras (m/s)	Results from two cameras (m/s)
2.2	6.52	6.41	6.35
9.6	7.98	7.70	8.60
34.6	9.29	9.03	8.85

Table 4
Results from the test conducted at CIBA at 15:35 – 02/04/2013.

Height (m)	Tower measurements (m/s)	Results from three cameras (m/s)	Results from two cameras (m/s)
2.2	5.65	5.61	5.58
9.6	7.24	7.35	7.40
34.6	8.67	8.48	8.43

Table 5
Comparison between anemometer and bubble tracking results for wind speed.

Date	Time (local)	Anem. (m/s)	Bub. (m/s)	Dif. (m/s)	Rel. error (%)
16-05-2012	13:10	2.36	2.38	0.02	1
16-05-2012	14:30	1.77	2.26	0.49	28
16-05-2012	15:30	1.69	1.99	0.30	18
16-05-2012	16:46	3.24	3.54	0.30	9
17-05-2012	13:09	3.40	3.56	0.16	5
01-06-2012	09:00	2.04	2.20	0.16	8
01-06-2012	09:25	2.66	2.74	0.08	3
01-06-2012	11:34	2.63	2.69	0.06	2
01-06-2012	12:44	2.98	3.18	0.20	7
08-06-2012	9:57	2.40	2.48	0.08	3
08-06-2012	11:15	1.06	1.28	0.22	21
08-06-2012	12:27	2.30	2.41	0.11	1

make the clusters good tracer particles for atmospheric average airfields.

3.2. *Analysis of wind profiles at atmospheric research centre*

Several tests have been carried out at the Centre for Low Atmosphere Research (CIBA) located in the northwest of Spain in an area of low roughness without edifications or remarkable surface features. The facility is suitable for experimental studies of the atmospheric boundary layer due to a 100 m meteorological tower, which is equipped with an anemometer at four different heights to obtain information about wind speed and direction. The results of the tests are summarised in

Table 6
Comparison between anemometer and bubble tracking results for wind direction.

Date	Time (local)	Anem. (deg)	Bub. (deg)	Dif. (deg)
16-05-2012	13:10	115	124	9
16-05-2012	14:30	116	124	8
16-05-2012	15:30	137	140	3
16-05-2012	16:46	90	78	−12
17-05-2012	13:09	198	191	−7
01-06-2012	09:00	356	2	6
01-06-2012	09:25	14	0	−14
01-06-2012	11:34	11	10	−1
01-06-2012	12:44	19	22	3
08-06-2012	9:57	271	263	−8
08-06-2012	11:15	240	258	18
08-06-2012	12:27	40	40	0

Tables 1 and 2, which show data from the 2nd, 3rd, and 12th of April 2012.

The differences between the calibrated anemometers and the proposed method have been compared to check the performance of the system, with the following results for RMS error at different heights:

- 0.28 m/s at 2.2 m height.
- 0.31 m/s at 9.6 m height.
- 0.31 m/s at 34.6 m height.

There is a difference in the sampling period of each system that could partially explain these differences. The anemometer samples every two seconds whereas the bubble tracking system provide data every 0.78 s. Also, these data do not correspond to fixed positions in the space, so only samples which were close to the anemometer position have been considered. Finally 5-min averages are compared for both the anemometer and the bubbles. Fig. 10 shows representative profiles obtained by the bubble tracking mechanisms compared to the data from the tower. Although it could seem that the area-sampling is less intuitive, it is quite common to take advantage of the wider coverage offered by this kind of sampling to improve the performance of meteorological codes.

Those tests carried out with three cameras, instead of only two, offer a series of operational and performance advantages:

- The accuracy of the results inversely depends on the distance between the cameras and the bubble clusters; so having three cameras allows one to ensure that the bubble cluster always approaches at least two cameras.
- The lines of sight of the cameras are more independent, with the triangulation algorithm being more robust.

- The system is able to perform properly under different wind conditions with no need for camera displacements or active pointing.
- Global accuracy is improved according to the results presented in Tables 3 and 4, where the measurements provided by the system with three cameras improve those achieved when only two of them are available.

The figures evidence a good correlation between the profiles, with the most relevant conclusions given as follows:

- This system has been validated for heights up to 40 m. Higher altitudes can be easily reached because there were no reported misdetected targets in the images; however, some bubbles abandoned the lateral fields of view, moved by strong winds after reaching those altitudes. Should more cameras be installed or their optics rearranged, the problem would be solved and a greater height range would be reached.
- These tests were also carried out during very windy and gusty conditions. This is the reason for the oscillation that occurred along the height, causing slightly deviations from the logarithmic profile. Even in these conditions, the system performed successfully.
- The turbulence intensity, calculated as the velocity deviation divided by the mean velocity, has reached almost the same value as that measured by the anemometers, very close to 0.15 at 10 m along the whole campaign.

3.3. Tests in the airfield

Additional experiments were developed in an airfield of the Spanish Air Force located in *La Virgen del Camino*, *León* (42°35′13″ N, 5°39′17″ W), where the prototype was also deployed. The test site was located close to the runway, where the roughness of the surrounding terrain is very low with little or no obstacles.

In this case, an anemometer tower was obviously not available, so the accuracy of the system could only be evaluated thanks to the measurements obtained by the meteorological stations deployed, validated by the aerodrome official meteorological service. The anemometers were located 6 m height, collecting continuous wind data during the whole validation campaign. These data (ground truth) could be compared to the output of the bubble tracking system, as given in Tables 5 and 6.

In this case, the bubble tracking system shows great performance; the root mean square error was calculated taking into

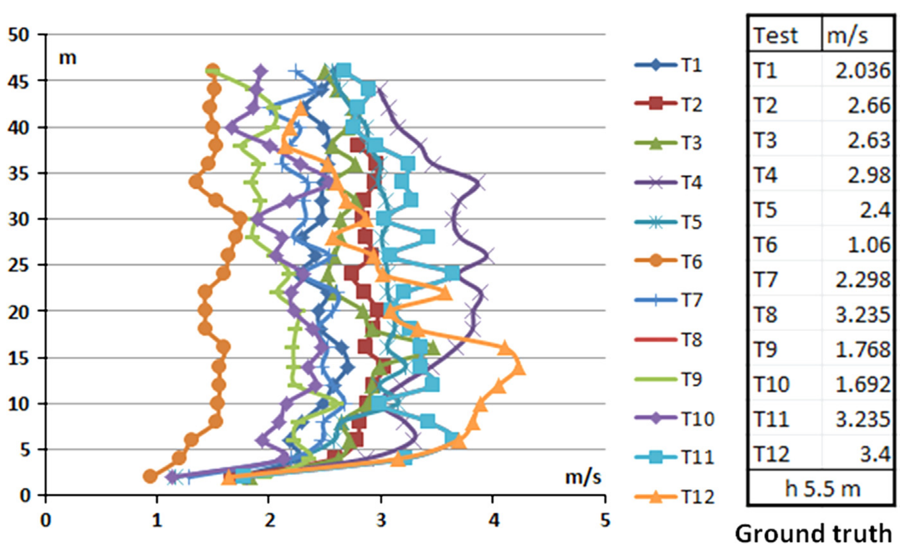


Fig. 11. Wind speed profiles obtained during the test campaign by means of the bubble tracking system.

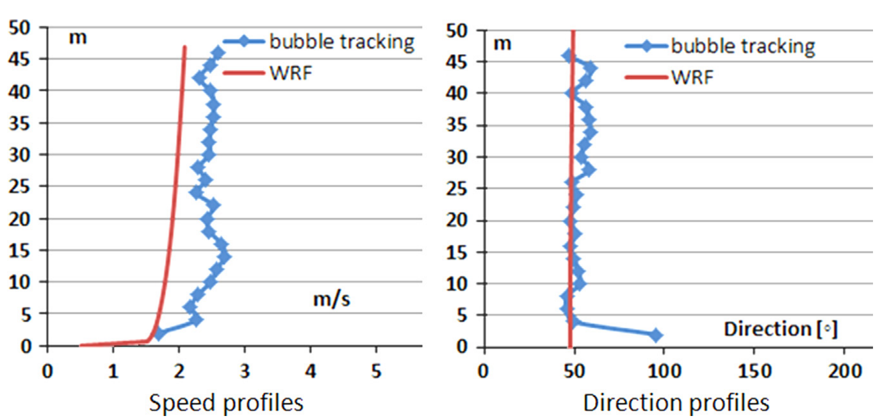


Fig. 12. Results of test T6 obtained from the bubble tracking system and the WRF.

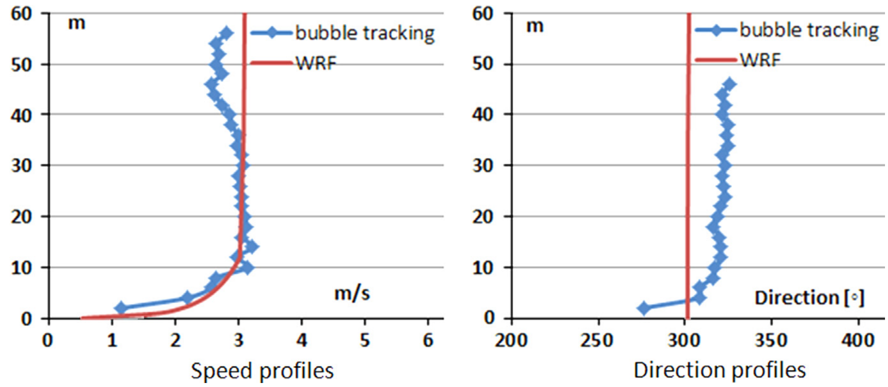


Fig. 13. Results of test T10 obtained from the bubble tracking system and the WRF.

account the difference between the measurements and ground truth for each test, with the result being as little as 0.22 m/s. The same process was applied for wind direction with a result of 9°.

The proposed system is capable of reproducing the vertical profile of the wind speed and direction. The previous section demonstrated that the accuracy at 6 m height was good enough. Then, according to the numerical sensitivity tests already referred during tests at CIBA, it can be stated that once the system is performing well at a certain point, its accuracy is maintained for enough time to complete the vertical profile with no significant performance degradation. The profiles measured during the test campaign are displayed in Fig. 11. From test number 2 to test number 5 the velocity decreases with height over a certain altitude range. This phenomenon is explained by the meteorological conditions at the time of the tests, a sunny and very hot day, when the temperature of the runway rises a lot and produces a strong convective motion with low horizontal speeds. The remaining tests were carried out earlier in the morning or under cloudy conditions, when the runway was not so hot, and the convective motion was moderate or null. In these cases the measured profile is quite similar to the common logarithmic one.

In addition, other numerical models have been used for calibration references in the airfield; this way, the measurements of the system under test can be compared to 3D found models developed from regional or global boundary and initial conditions. The model used was the Weather and Research Forecasting (WRF) with the Advanced Research WRF (ARW) solver, designed to be a flexible state-of-the-art atmospheric simulation system with proven accuracy [35]. Applying this procedure, some of the velocity profiles obtained during the tests are shown here and compared with the profiles predicted by the WRF for the wind speed and direction at that very location and date/hour. These data can be observed in Figs. 12 and 13.

The speed quickly grows with height, following a logarithmic law, until reaching an almost constant value. This shape is clearly visible in both profiles and the similarities between the measured profile and the forecast are obvious. Also, the measured and predicted wind directions match pretty well along the profile.

4. Conclusions

The technologies around the remote sensing of atmospheric wind profiles have been reviewed to highlight the feasibility of a new mechanism to estimate wind speed and direction in an affordable and safe manner. This method is, for certain applications, a reliable and low cost alternative to conventional ground sensors and remote sensing technologies.

Inspired by the PIV techniques and the use of balloons, the system releases lighter-than-air bubbles and, by means of a filtered triangulation process, it is able to determine instantaneous positions and velocity of the bubbles from conventional imagery. The system's performance was initially tested in synthetic scenarios, showing encouraging results, tuned by indoor test results and finally validated by field tests carried out in two different locations: an atmospheric research centre (CIBA) and an operational airfield. The first in-field validation included a comparison of the results of the new system with those provided by the calibrated anemometry equipment located at different heights in the CIBA facilities. For the airfield, the references were the in situ anemometer and the wind profiles predicted by highly validated numerical models. The wind speeds measured by the bubble tracking system during the test campaigns matched well with those given by the references, reaching accuracy goals initially established for the prototype version (0.4 m/s for wind speed and 15° for wind direction). Factors originating from such differences – sampling rate and measurement averaging methods – have been identified and discussed, proposing improvements for the operational versions of the system.

Obviously, before becoming a real alternative to traditional anemometry systems, the system will require more effort in data acquisition and processing, as well as automation; however, the results presented here are very encouraging. A detailed calibration process would also provide better accuracy, customising the parameters for each test location. Anyway, these initial results suggest that the proposed system allows an accurate measurement of low atmospheric winds in real time. The plan is to apply the concept to an airport area, providing timely data to air controllers and eventually pilots operating around; nevertheless, the system can be very useful in many other applications, mainly when the user cannot afford expensive instruments but when wind profile knowledge is valuable.

References

[1] Landberg L. Short-term prediction of the power production from windfarms. J Wind Eng Ind Aerodyn 1999;80:207–20.
[2] Van Nunen JWG, Persoon AJ. Investigation of the vibrational behaviour of a cable-stayed bridge under windloads. Eng Struct 1982;4:99–105.
[3] Gorlé C, van Beeck J, Rambaud P, Van Tendeloo G. CFD modelling of small particle dispersion: the influence of the turbulence kinetic energy in the atmospheric boundary layer. Atmos Environ 2009;43:673–81.
[4] Sanz-Andres A, Cuerva A. Pedestrian wind comfort: feasibility study of criteria homogenisation. J Wind Eng Ind Aerodyn 2006;94:799–813.
[5] José Meseguer Ruiz, Andrés Ángel Sanz, Perales José Manuel Perales, Carrión Santiago Pindado. Aerodinámica Civil: Cargas de viento en las edificaciones. Madrid: McGraw-Hill; 2001.
[6] Stefan Emeis, Münkel Christoph, Vogt Siegfired, Müller Wolfgang J, Schäfer Klaus. Atmospheric boundary-layer structure from simultaneous SODAR, RASS, and ceilometer measurements. Atmos Environ 2004;38:273–86.
[7] Johnson Hakeem K. Simple expressions for correcting wind speed data for elevation. Coast Eng 1999;36:263–9.

[8] Domínguez Diego. Improvements in the study and prediction of local wind fields, particularly in airport surroundings, with implication in air traffic safety [PhD thesis]; 2012.
[9] Meischner Peter. Weather radar: principles and advanced applications. Berlin: Springer; 2004.
[10] Newman JF, LaDue DS, Heinselman PL. Identifying critical strengths and limitations of current radar systems. In: 24th conference on severe local storms. Savannah, GA: American Meteorological Society; 2008.
[11] Weitkamp Claus. LIDAR: range-resolved optical remote sensing of the atmosphere. New York, USA: Springer; 2005.
[12] Fujii Takashi, Fukichi Tetsuo. Laser remote sensing. Boca Raton, FL, USA: CRT Press; 2005.
[13] Cimini Domenico, Marzano Frank S, Visconti Guido. Integrated ground-based observing systems. Berlin: Springer; 2010.
[14] Emeis Stefan. Surface based remote sensing of the atmospheric boundary layer. Dordrecht: Springer; 2011.
[15] Allaby Michael. Encyclopedia of weather and climate. New York: Facts on File; 2002.
[16] Mahapatra Pravas R. Aviation weather surveillance systems: advanced radar and surface sensors for flight safety and air traffic management. Reston, VI: American Institute of Aeronautics and Astronautics; 1999.
[17] Ahrens C Donald. Essential of meteorology. An invitation to the atmosphere. Belmont, USA: Cengage Learning; 2008.
[18] Naderi F, Freilich MH, Long DG. Spaceborne radar measurement of wind velocity over the ocean – an overview of the NSCAT scatterometer system. Proc. IEEE 1991;79(6):850–66.
[19] Nava Enzo, Stucchi Emanuele. Development of lasers for spaceborne Doppler wind lidar applications. Opt Lasers Eng 2003;39:255–63.
[20] Raffel M, Willert CE, Wereley ST, Kompenhans J. Particle image velocimetry – a practical guide. 2nd ed. Berlin: Springer; 2007.
[21] Corvaro F, Paroncini M. An experimental study of natural convection in a differentially heated cavity through a 2D-PIV system. Int J Heat Mass Transfer 2009;52(1–2):355–65.
[22] Cristina Sanjuan, Sánchez María Nuria, Heras Maria del Rosario, Blanco Eduardo. Experimental analysis of natural convection in open joint ventilated façades with 2D PIV. Build Environ 2011;46(11):2314–25.
[23] Troolin D, Longmire E. Volumetric velocity measurements of vortex rings from inclined exits. Exp Fluids 2010;48(3):409–20.
[24] Nuno Serra, Semiao Viriato. Characterization of non-isothermal flows typical of built environments in a laboratory scale model. Part I – experiments with 3D PIV. Build Environ 2013;68:225–38.
[25] Kalmbach A, Breuer M. Experimental PIV/V3V measurements of vortex-induced fluid–structure interaction in turbulent flow—a new benchmark FSI-PfS-2a. J Fluids Struct 2013;42:369–87.
[26] Domínguez Diego, Jesús Gonzalo, Deibi López. A wind speed profile measurement method based on free bubble tracking in the lower atmosphere. Flow Meas Instrum 2013;34:134–41.
[27] Wilkerson Thomas D, Marchant Alan B, Apedaile Thomas J. Wind field characterization from the trajectories of small balloons. J AtmosOcean Technol 2012.
[28] Toshio Koizumi, Ueda Hiroshi, Matsushima Dai. Development of a wind observation system utilizing simplified aerial photogrammetry(3) – the measurement of wind flow by phototheodolite and soap bubbles. J Wind Eng 2011;36(1):1–12.
[29] Kawasaki Hideaki, Toshio Koizumi, Kazuhiro Matsuda. Development of a wind observation system using photogrammetry. In: XXII ISPRS congress. Melbourne, Australia; 2012.
[30] Domínguez Diego, Jesús Gonzalo, Deibi López. Numerical modelling of a wind profiler system based on bubble tracking. Math Comput Model Dyn Syst 2014;20(3):209–23.
[31] Isenberg Cyril. The science of soap films and soap bubbles. New York: Dover Publications; 1992.
[32] Kalman RE. A new approach to linear filtering and prediction problems. J Basic Eng 1960;82D.
[33] Crassidis JL, Markley FL, Cheng Y. Survey of nonlinear attitude estimation methods. J Guid Control Dyn 2007;30:12–28.
[34] Douce Arnaud, Adam M Johansen. A tutorial on particle filtering and smoothing: 15 years later. In: Oxford handbook of nonlinear filtering, 2011, Oxford University Press, Oxford.
[35] Rafael Borge, Alexandrov Vassil, Del Vas Juan José, Lumbreras Julio, Rodríguez Encarnación. A comprehensive sensitivity analysis of the WRF model for air quality applications over the Iberian Peninsula. Atmos Environ 2008;42:8560–74.
[36] Grewal MS, Andrews AP. Practical considerations. in: Kalman filtering: theory and practice using MATLAB®. 3rd ed. Hoboken, NJ, USA: John Wiley & Sons, Inc.; http://dx.doi.org/10.1002/9780470377819. [chapter 8].